

# DETECTING LAND COVER CHANGE USING A SLIDING WINDOW TEMPORAL AUTOCORRELATION APPROACH

<sup>†‡</sup>W. Kleynhans, <sup>†‡</sup>B.P Salmon, <sup>\*</sup>J.C. Olivier, <sup>‡</sup>F. van den Bergh, <sup>‡</sup>K. J. Wessels, <sup>‡</sup>T. Grobler

<sup>†</sup>Department of Electrical, Electronic and Computer Engineering, University of Pretoria, South Africa

<sup>‡</sup>Remote Sensing Research Unit, Meraka Institute, CSIR, Pretoria, South Africa  
wkleynhans@csir.co.za

<sup>‡</sup>Defense, Peace, Safety and Security Unit, Meraka Institute, CSIR, Pretoria, South Africa

<sup>\*</sup>School of Engineering, University of Tasmania, Australia

## ABSTRACT

There has been recent developments in the use of hyper-temporal satellite time series data for land cover change detection and classification. Recently, an Autocorrelation function (ACF) change detection method was proposed to detect the development of new human settlements in South Africa. In this paper, an extension to this change detection method is proposed that produces an estimate of the change date in addition to the change metric. Preliminary results indicate that comparable accuracy is achievable relative to the original formulation, with the added advantage of providing an estimate of the change date.

## 1. INTRODUCTION

Anthropogenic land cover change has a major impact on hydrology, climate and biodiversity [1]. The most pervasive form of land-cover change in South Africa is human settlement expansion. In many cases, new human settlements are informal and occur in areas that were previously covered by natural vegetation. There has been recent developments in the use of hyper-temporal satellite time series data for land cover change detection and classification in Southern Africa. Specifically, an Autocorrelation Function (ACF) change detection method was recently proposed to detect the development of new human settlements in South Africa [2, 3, 4]. This method is based on MODIS time-series data, which have been proven to be separable for the land cover classes considered in this study [5]. The method uses the ACF of this MODIS time-series to indicate the level of stationarity of the time-series, which is then used as a measure of land cover change. It was previously shown that new settlement developments could be efficiently detected using specific MODIS bands [6]. The appropriate band, ACF lag and correlation value that is used as a change index is determined by means of simulation. The method calculates the ACF of the entire time-series and produces a single change index which, when compared to a

threshold value (determined by simulation) yields a change or a no-change decision [6].

In the original formulation [6], the entire time-series (spanning eight years) was used as input, resulting in a change alarm for the entire period with no indication of when the change occurred. The objective of this paper is to extend this method by using a temporal sliding window approach in order to determine the date of change. Apart from only providing a change alarm, the proposed method would then also provide information on the timing of the change, i.e. gives an indication of when the change occurred. Preliminary results show that by using the correct window length and threshold, very comparable detection accuracy can be achieved relative to that which was achievable using the original formulation, with the added advantage of providing an estimate of the change date.

## 2. DATA DESCRIPTION

### 2.1. Study Area

The Gauteng province is located in northern South Africa and because of a high level of urbanization it has seen significant human settlement expansion during the 2001 and 2008 period. A total area of approximately 17000 km<sup>2</sup> (centered around 26°07'29.62''S, 28°05'40.40''E) was considered. The time-series for all seven MODIS land bands, as well as NDVI derived from 8-day composite, 500 m, MCD43 BRDF-corrected, MODIS data was used for the period 2001/01 to 2008/01. A dataset of no-change pixel time-series ( $n=964$ ) consisting of natural vegetation ( $n=592$ ) and settlement ( $n=372$ ) pixels, were identified by means of visual interpretation of high resolution Landsat and SPOT images in 2000 and 2008 respectively. Examples of confirmed settlement developments during the study period were also obtained by means of visual interpretation of high resolution Landsat and SPOT images in 2000 and 2008 respectively.



**Fig. 1.** QuickBird image acquired in 2002 (left image) and 2007 (right image) respectively. The polygon on the left in both images is the outline of a 500 m MODIS pixel in an area that changed from natural vegetation to settlement while the polygon on the right in both images is the outline of a 500 m MODIS pixel in an area that remained naturally vegetated. (courtesy of Google<sup>TM</sup>Earth)

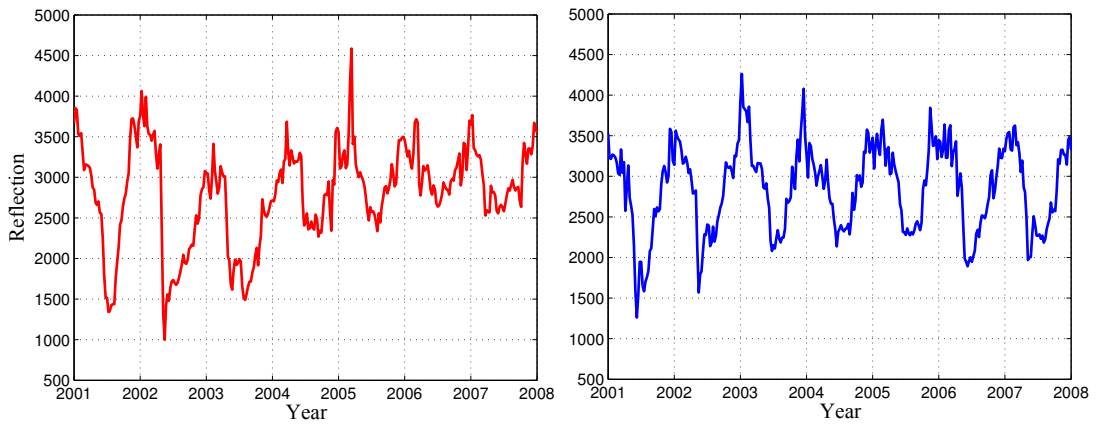


**Fig. 2.** Change (left) and no-change (right) MODIS band 4 time-series of the polygons shown in figure 1

All settlements identified in 2008 were referenced back to 2000 and all the new settlement polygons were mapped and the corresponding MODIS pixels ( $n=181$ ) were identified. The real change pixels and remaining pixels of the no-change dataset ( $n=482$ ) were used in an unsupervised operational mode to test the change detection capability of the method.

### 3. METHODOLOGY

#### 3.1. Temporal ACF method

The Temporal ACF method proposed in [6] uses a two stage approach. Firstly, the band, lag and threshold selection is done using a simulated change dataset together with the no-change dataset. Second, the aforementioned parameters are used in an unsupervised manner to detect change. Assume that a MODIS time-series is expressed as

$$\mathbf{X} = X_n, n \in \{1, 2, \dots, N\}, \quad (1)$$

where  $X_n$  is the observation from an arbitrary spectral band

at time  $n$  and  $N$  is the number of time-series observations available.

The ACF for time-series  $\mathbf{X} = [X_1, X_2, \dots, X_N]$  can then be expressed as

$$R(\tau) = \frac{E[(X_n - \mu)(X_{n+\tau} - \mu)]}{\text{var}(\mathbf{X})}, \quad (2)$$

where  $\tau$  is the time-lag and  $E$  denotes the expectation. The mean of  $\mathbf{X}$  is given as  $\mu$  and the variance, which is used for normalization, is given as  $\text{var}(\mathbf{X})$ . Figure 1 shows an example of a change and no-change MODIS pixel with figure 2 showing the corresponding MODIS time-series for each of these pixels. The ACF of the time-series given in figure 2 is shown in figure 3. It is clear that the no-change pixel has a symmetrical form relative to the  $R(\tau) = 0$  axis, whereas the change pixel shows a strong non-symmetrical property. The reason for this is the stationarity requirement of the ACF in (2). The mean and variance of the time-series of  $\mathbf{X}$  in (2)

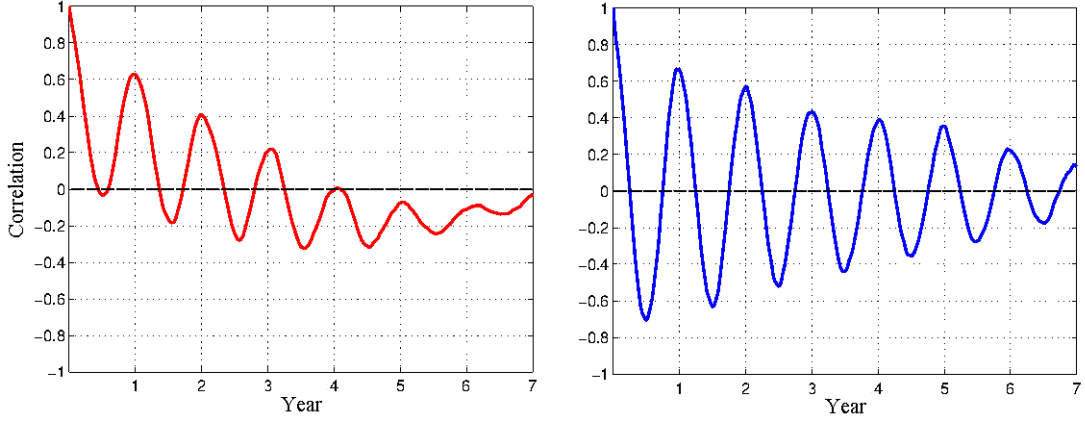


**Fig. 3.** ACF of the change (left) and no-change (right) MODIS pixel's time-series shown in figure 2.

is required to remain constant through time to determine the true ACF of the time-series. The inconsistency of the mean and variance typically associated with a change pixel's non-stationary time-series thus becomes apparent when analyzing the ACF of the time-series. The change metric is thus simply equivalent to the temporal correlation at a specific lag ( $\tau$ ) given as

$$R(\tau) = \delta_\tau. \quad (3)$$

It is clear that the distribution of  $\delta_\tau$  in the case of change and no-change, will vary for different values of  $\tau$ . The aim is thus to determine the value of  $\tau$  in  $\delta_\tau$  that will result in the most separable distributions between  $\delta_\tau$  for the change and no-change case. The value of the optimal threshold ( $\delta_\tau^*$ ) also needs to be determined. The aim is to determine the time-lag ( $\tau$ ) and threshold ( $\delta$ ) which provide the best separation between the ACF of a change and no-change pixel time-series taken from the simulated change and no-change datasets respectively. After the off-line optimization phase is complete, the resulting parameters are used to run the algorithm in an unsupervised manner for the entire study area. A pixel is labeled as having changed by evaluating the following,

$$\text{Change} = \begin{cases} \text{true} & \text{if } R(\tau) > \delta^* \\ \text{false} & \text{if } R(\tau) < \delta^* \end{cases}$$

where  $R(\tau)$  is the ACF evaluated at lag  $\tau$  and  $\delta^*$  is the decision threshold. The value of  $\tau$  and  $\delta^*$ , was provided in the off-line optimization phase.

### 3.2. Sliding Window Temporal ACF method

The sliding window extension to (2) can be expressed as

$$R(\tau, i) = \frac{E[(X_n - \mu)(X_{n+\tau} - \mu)]}{\text{var}(\mathbf{X})}, \quad (4)$$

where  $\mathbf{X} = X_n$   $n \in \{i, i+1, \dots, i+w-1\}$ ,  $i \in \{1, 2, \dots, N-w+1\}$  and  $w$  is the window length. Unlike the lag selection

done in [6], a summation of the first 23 lags was performed as preliminary simulations showed only a marginal reduction in accuracy when summing over the first 23 lags as opposed to explicitly selecting a value of  $\tau$ . This also reduces the number of parameters to be optimized, thus making the method more general.

$$\delta_i = \sum_{\tau=1}^{23} R(\tau, i). \quad (5)$$

A pixel is labeled as having changed by evaluating the following,

$$\text{Change} = \begin{cases} \text{true} & \text{if } \max(\delta_i) > \delta^* \\ \text{false} & \text{if } \max(\delta_i) < \delta^* \end{cases}$$

If change is true, the change date then simply corresponds to the index associated with  $\max(\delta_i)$ . The value of  $\delta^*$  and optimal window size is determined by means of simulation.

## 4. RESULTS

Figure 4 shows the overall accuracy as a function of the change detection delay for different window sizes and thresholds. The overall accuracy was determined by combining the change detection accuracy with the false alarm rate to create a single accuracy metric. The false alarm rate was determined by running the algorithm on a no-change dataset, whereas the change detection accuracy was determined by means of an instantaneous change from natural vegetation to a settlement, effectively splicing a natural vegetation pixel's time-series with a close proximity settlement pixel's time series. It is clear that the window size that is chosen has a dramatic effect on the overall change detection accuracy and detection delay. A choice of which window size and threshold to choose is based on the specific user requirement. If, for example, a high overall accuracy is more important than the detection delay, a larger window should be selected. For example, a greater than 75% overall accuracy will require a window length of 80

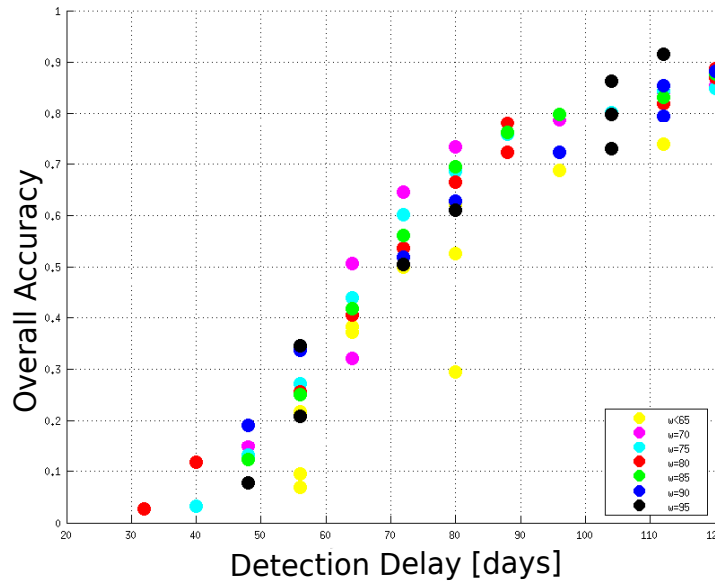


**Fig. 4.** Overall accuracy as a function of the detection delay using a range of window sizes and threshold values, the color of the dots indicate the window size measured in number of 8-day MODIS samples.

or 85 MODIS 8-day samples yielding a best case detection delay in the order of 87 days (figure 4). When detection delay should be minimal, a smaller window size can be chosen at the expense of the change detection accuracy. For example, a shorter than 70 day detection delay will require a window length in the order of 70 MODIS 8-day samples yielding a best case overall accuracy of 50% (figure 4). The simulated change framework presented here gives the operator an idea of the window-size, detection delay and detection accuracy trade-off by measuring the the delay from the point at which the simulated change was induced.

## 5. CONCLUSION

In this paper, an extension is proposed to the work done in [6]. The original formulation is a threshold based change alarm that uses an ACF of an entire time-series to infer a change index and uses a simulated change and no-change dataset to determine an optimal band lag and threshold. The method proposed in this paper is an extension to the aforementioned which provides an estimate of the change date using a temporal sliding window ACF approach. The optimal window size and threshold is obtained by means of simulated change and can be selected based on the users specific requirements.

## 6. REFERENCES

[1] R. T. Watson, *Land Use, Land-Use Change and Forestry*, Cambridge University Press, Cambridge, England, 2000.  
 [2] B.P. Salmon, J.C. Olivier, K.J. Wessels, W. Kleynhans, F. van den Bergh, and K.C. Steenkamp, "Unsupervised

land cover change detection: Meaningful sequential time series analysis," *Selected Topics in Applied Earth Observations and Remote Sensing, IEEE Journal of*, vol. 4, no. 2, pp. 327 –335, june 2011.

[3] W. Kleynhans, J.C. Olivier, K.J. Wessels, F. van den Bergh, B.P. Salmon, and K.C. Steenkamp, "Improving land cover class separation using an extended kalman filter on modis ndvi time-series data," *Geoscience and Remote Sensing Letters, IEEE*, vol. 7, no. 2, pp. 381 –385, april 2010.  
 [4] W. Kleynhans, J.C. Olivier, K.J. Wessels, B.P. Salmon, F. van den Bergh, and K. Steenkamp, "Detecting land cover change using an extended kalman filter on modis ndvi time-series data," *Geoscience and Remote Sensing Letters, IEEE*, vol. 8, no. 3, pp. 507 –511, may 2011.  
 [5] T. L. Grobler, E. R. Ackermann, J. C. Olivier, A. J. van Zyl, and W. Kleynhans, "Land-cover separability analysis of modis time-series data using a combined simple harmonic oscillator and a mean reverting stochastic process," *Selected Topics in Applied Earth Observations and Remote Sensing, IEEE Journal of*, 2012,doi:10.1109/JSTARS.2012.2183118.  
 [6] W. Kleynhans et al., "Land cover change detection using autocorrelation analysis on MODIS time-series data: Detection of new human settlements in the Gauteng province of South Africa," *Selected Topics in Applied Earth Observations and Remote Sensing, IEEE Journal of*, 2012, doi:10.1109/JSTARS.2012.2187177.